SALT-INDUCED MESOSCOPIC AGGREGATION OF POLYVINYL ALCOHOL IN AQUEOUS SOLUTION

by

Phuong Diep

Submitted in partial fulfillment of the

requirements for Departmental Honors in

the Department of Chemistry

Texas Christian University

Fort Worth, Texas

May 5th 2014

SALT-INDUCED MESOSCOPIC AGGREGATION OF POLYVINYL ALCOHOL IN AQUEOUS SOLUTION

Project Approved:

Supervising Professor: Dr. Onofrio Annunziata, PhD

Department of Chemistry

Dr. Giridhar R. Akkaraju, PhD

Department of Biology

Dr. Julie A. Fry, PhD

Department of Chemistry

ABSTRACT

Polyvinyl alcohol (PVA) is a biocompatible and inexpensive nonionic polymer used in several industrial and pharmaceutical applications.[1,2] One important property of the aqueous solutions of this polymer is the formation of hydrogels.[3] These are usually obtained by lowering temperature.[3] Although there is extensive fundamental research on PVA hydrogel materials, the formation and characterization of mesoscopic PVA hydrogels, i.e. PVA nanoparticles, in solution have hardly been explored. Here, we have successfully induced the formation of PVA nanoparticles by using aqueous salts. The choice of salts in our work was motivated by the extensive use of these additives to induce protein precipitation from aqueous solutions.[4] Moreover, salts have been ranked according to their effectiveness in precipitating proteins. This ranking is known as the Hofmeister series.[4] In this series, sulfates and chlorides are known to be strong and mild precipitating agents respectively. On the other hand, thiocyanates are known to protect proteins from precipitation. In our experiments with PVA, we found that Na_2SO_4 induces extensive macroscopic aggregation of this polymer in water. On the other hand, no aggregation was observed in the presence of NaSCN. Interestingly, in the case of NaCl, a slow PVA aggregation process occurred, leading to the formation of opaque samples. The NaCl-induced aggregation of PVA was investigated using Dynamic Light Scattering (DLS). Our results revealed that PVA-water solutions contain a small amount of aggregates with radius of 30 nm. In the presence of NaCl, these aggregates grow and reach a radius of about 100 nm. To explain our experimental findings a quantitative kinetic model was developed.

ACKNOWLEDGEMENTS

I want to say my dearest thanks to Dr. Onofrio Annunziata and Viviana Costa for guiding me through my experiments from the beginning to the end. I want to say thanks also to Dr. Julie Fry and Dr. Giridhar R. Akkaraju for revising my thesis.

TABLE OF CONTENTS

INTRODUCTION

Polyvinyl Alcohol (PVA)

Polyvinyl alcohol (PVA) is a biocompatible and inexpensive nonionic polymer used in several industrial and pharmaceutical applications.[1,2] PVA-water mixtures are known to undergo physical gelation, a property that makes PVA one of the most valuable polymers for the production of films and hydrogels with excellent mechanical properties.[3] The association of PVA chains is induced by hydrogen bonds between hydroxyl groups and Van der Waals interactions between hydrocarbon polymer backbones.[1] PVA-water gels have been investigated using several experimental techniques.[2-3] These studies have revealed that PVA hydrogels are bicontinuous networks in which the PVA-rich phase consists of crystalline-like ordered nanoclusters, denoted as *crystallites*, embedded in a PVA amorphous matrix (see Fig.1).

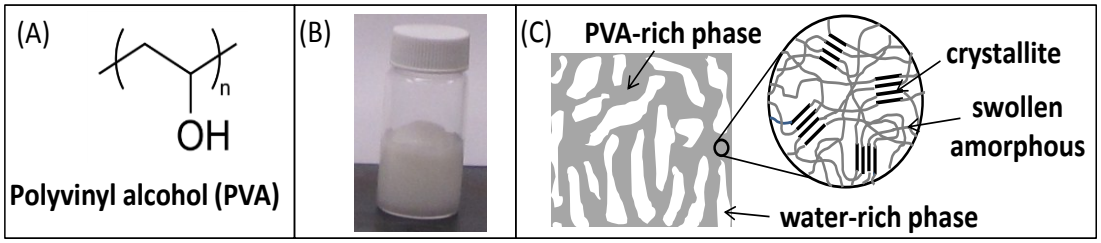

Figure 1. (A) Chemical Structure of PVA. (B) Sample of atactic PVA-water hydrogel (MW: 100 kg/mol, 14% w/w) prepared in the PI's lab. Hydrogels were prepared through cryogelation, i.e. freezing-thawing polymer aqueous solutions.[3] (C) Bicontinuous structure of PVA hydrogels with PVA-rich and water-rich phases. As shown by X-ray diffraction, the PVA-rich phase consists of PVA crystallites embedded in a PVA swollen amorphous matrix.[4] Thus PVA hydrogels exhibit a semicrystalline character despite the lack of polymer stereoregularity. The average diameter of the crystallites was found to be 7 nm by small angle neutron scattering.

PVA and its hydrogels have largely been used successfully in many biomedical applications. For example, PVA hydrogels have been used for contact

lenses, the lining for artificial hearts, and drug- delivery applications.[5] However, these materials do not fall within the scope of nanomedicine due to their large sizes. Currently, these PVA gels are typically obtained through cryogelation, which is a process of freezing and thawing of polymer aqueous solutions to yield PVA-based hydrogels with excellent mechanical properties, biocompatibility and stability.[5]

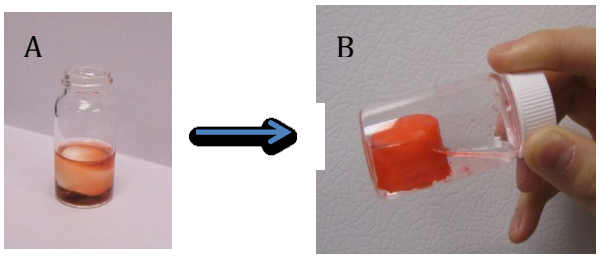

ure 2. Ability of PVA to adsorb Congo Red. (A). Pictures taken at TCU. The picture on the left was taken immediately after the addition of Congo Red to the gel–water suspension. The characteristic color of PVA is white. (B) The picture on the right was taken after one day. The PVA gel has adsorbed most of the red dye as we can appreciate from the color of the gel. Correspondingly, the surrounding fluid became colorless.

In addition to its ability to form hydrogel, PVA also has the ability to adsorb dyes. For example: Congo Red (shown in Figure 2). This property of PVA allows us to apply these materials to the removal of several organic molecules from aqueous environments. In addition, PVA can also be used as a potential scaffold for many functional organic molecules such as porphyrins.[6]

Although there is extensive fundamental research on PVA macroscopic hydrogels, the formation and characterization of PVA nanoparticles in solution has hardly been explored.[7-11] Hence, being able to control and to characterize the formation of PVA mesoscopic aggregates (i.e. nanoparticles) will open up new venues for various applications in nanotechnology. Specifically, related studies would potentially lead to the preparation of novel nanomaterials in which PVA aggregates act as scaffolds for small molecules that are biologically and chemically active, with applications in the fields of catalysis, photonics and medicine.[12] Hence,

the objective of this research is to prepare novel polymeric nanoparticles by inducing polymer aggregation in aqueous salt solutions.

Hofmeister Series

One important way to prepare nanoparticles is to induce the aggregation of synthetic polymer chains in solution. Interestingly, salts have been used to induce the aggregation of biological polymers such as proteins[12] in water. Salt effectiveness to induce aggregation and crystallization of protein can be ranked according to the Hofmeister series.[12] (Figure 3) It is also known that salt effectiveness significantly depends more on the nature of the anion than on the nature of the cation.

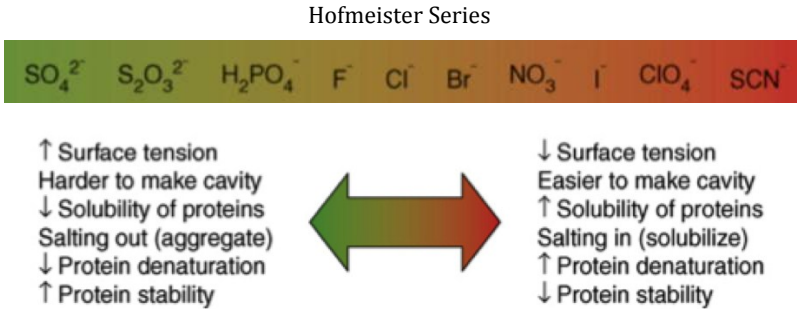

Figure 3. The anion Hofmeister Series ranks the effectiveness of salt anions in precipitating proteins. The anions: SO_4^{2-}, Cl^-, SCN^-, which are located on the left, middle and right of the series, were chosen in this investigation.

According to the series, sulfate salts are strong precipitating agents while chloride salts have a relatively mild effect on the aggregative properties of macromolecules. On the other hand, thiocyanate salts are expected to inhibit aggregation. By performing our experiment with these three different types of salt, we were able to identify a salt that induces PVA mesoscopic aggregation in aqueous solutions.

Dynamic Light Scattering (DLS)

The technique we used to characterize the kinetics of PVA aggregation and the size of the formed PVA mesoscopic aggregates is Dynamic Light Scattering (DLS). This technique is typically utilized to measure diffusion coefficients (D) of polymers, proteins and aggregates in solution. DLS is a non-invasive technique, as it does not require staining or isolating the particles of interest from their surrounding medium. This is especially important when kinetic experiments are performed. The value of the diffusion coefficient collected from DLS can then be converted to the radius of the particle using the Stoke–Einsten equation as follows:[13]

$$R = \frac{k_b T}{6\pi\eta D} \quad (1)$$

with R being the radius of particle, k_b the Boltzman constant, T as temperature of the experiment, and η as viscosity of the PVA-free mixtures.

The scheme of the DLS apparatus is described in Figure 4 below. Light coming from a laser passes through a cell containing the PVA aggregates in aqueous solution. Light is then scattered at 90° and collected by a detector. The data is then analyzed by a computer and gives us diffusion coefficient as a final value.

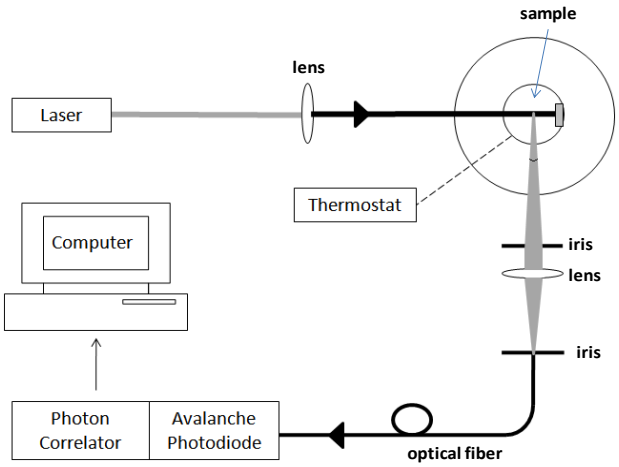

Figure 4. Light coming from a laser is sent to a cell containing the PVA aggregates in aqueous solution. Light scattered at 90° from the sample is collected by a detector and the results are analyzed by a computer. The DLS photodetector records the light-scattering intensity as a function of time. Due to erratic movements of aggregates (Brownian motion), the intensity scattered by these particles fluctuates as a function of time.

If different types of particles are present in a sample (e.g. polymer chains and larger aggregates), DLS can be used to extract particle-size distributions. If the amount of aggregates increases with time, then these distributions are time-dependent, and can be used to extract valuable kinetic information on the aggregation rate.

EXPERIMENTAL SECTION

Materials

The materials used in the experiment are Polyvinyl Alcohol (nominal molecular weight: 16 kg/mol), NaCl, Na_2SO_4 and NaSCN. These materials are commercially available (from Sigma-Aldrich). Deionized water available in our laboratory was further purified through a four-stage water-purification system.

Solution Preparation

For the DLS experiments, PVA-NaCl-water solutions were prepared by weighing (±0.0001 g) different amounts of PVA-water (2.0% w/w) and NaCl-water

(25% w/w) stock solutions. Our typical NaCl final concentration corresponds to a molality of 2.0 mol/kg.

Using these stock solutions and water, our final solutions were prepared at the following concentrations (w/w): 1.1% PVA, 0.8% PVA and 0.5% PVA. It is important to remark that PVA-water stock solutions were initially filtered using 0.2-μm filters.. The final solutions were then filtered again using 0.1-μm filters to eliminate small amounts of very large aggregates and dust particles before DLS experiments were started.

Dynamic Light Scattering (DLS)

Measurements of DLS were performed at 25.0 ± 0.1 ºC and 37.0 ± 0.1 ºC. The experiments were performed on a light-scattering apparatus built using the following main components: He-Ne laser (35 mW, 632.8 nm, Coherent Radiation), manual goniometer and thermostat (Photocor Instruments), multi-tau correlator, APD detector and software (PD4042, Precision Detectors). All measurements were performed at a scattering angle of 90°. The dynamic-light-scattering correlation functions were analyzed using a regularization algorithm (Precision Deconvolve 32, Precision Detectors). The mean apparent hydrodynamic radius, $< R^{-1} >^{-1}$, was calculated using the Stokes-Einstein equation (1), where η is the viscosity of the PVA-free mixtures. We have used $\eta = 1.073 \times 10^{-3}\ \mathrm{kg\,m^{-1}s^{-1}}$ for NaCl 2.0 mol/kg H_2O at 25 ºC, and $\eta = 0.831 \times 10^{-3}\ \mathrm{kg\,m^{-1}s^{-1}}$ at 37 ºC. Note that the mean diffusion coefficient can be also calculated for individual peaks in bimodal distributions: $< R_1^{-1} >^{-1} = k_B T / (6\pi\eta < D_1 >)$, where R_1 and D_1 are the mean radius and diffusion

coefficient for a single PVA chain, and $< R_m^{-1} >^{-1} = k_B T / (6\pi\eta < D_m >)$ for a PVA aggregates consisting of m PVA chains, where R_m and D_m are the mean radius and diffusion coefficient for the aggregate.

Turbidity Measurements

Sample turbidity was measured as a function of temperature. A turbidity meter was built by using a programmable circulating bath (1197P, VWR) connected to a homemade optical cell where the sample is located. The temperature at the sample location was measured by using a calibrated thermocouple (± 0.1 ºC). Light coming from a solid-state laser (633 nm, 5 mW, Coherent) goes through the sample with optical path $L = 0.40\,\text{cm}$ and the transmitted intensity, I, is measured using a photo-diode detector and a computer-interfaced optical meter (1835-C, Newport). For our initially transparent sample, the transmitted intensity, I_0, was measured. The temperature of the water bath was slowly increased (0.5 ºC/min) and the turbidity $\tau = (1/L)\,\log(I_0 / I)$ was plotted as a function of temperature, T.

Light Microscopy

Samples containing PVA aggregates were observed under a light microscope (Axioskop 40, Zeiss) using phase-contrast microscopy. Images were taken using a digital camera (Axiocam MRc, Zeiss) interfaced by a computer with software (Axiovision AC 4.5, Zeiss).

RESULTS

Effect of salt type on PVA aggregation

Our investigation started by exploring the effect of salt type on the PVA aggregation. Specifically, we have performed experiments with three different salts at room temperature (22-23 °C). Our results are shown in Figure 5. In these experiments, we found that sodium sulfate (Na_2SO_4) quickly induces precipitation with the formation of very large PVA aggregates (> size of the order of 1 mm). On the other hand, PVA solutions under the effect of sodium thiocyanate (NaSCN) did not produce aggregates (solutions remain transparent after one month). This confirms that NaSCN does not induce aggregation. It is actually expected that this salt inhibits PVA from aggregating, according to the Hofmeister series. Thus, we turned our attention to NaCl, a mild precipitating agent, with the chloride ion roughly located at the midpoint of the Hofmeister series. Our preliminary experiments show that PVA solutions in the presence of NaCl (≈2M) were observed to become opaque over time in the order of days. However no macroscopic precipitation could be detected after one month by visual inspection of the samples. Thus, this approach is very promising because sample opacification without precipitation can be associated with the formation of mesoscopic aggregates (i.e. PVA nanoparticles with diameter less than 1 μm) suspended in water. To characterize the size and kinetics of this aggregation process, we used Dynamic Light Scattering (DLS).

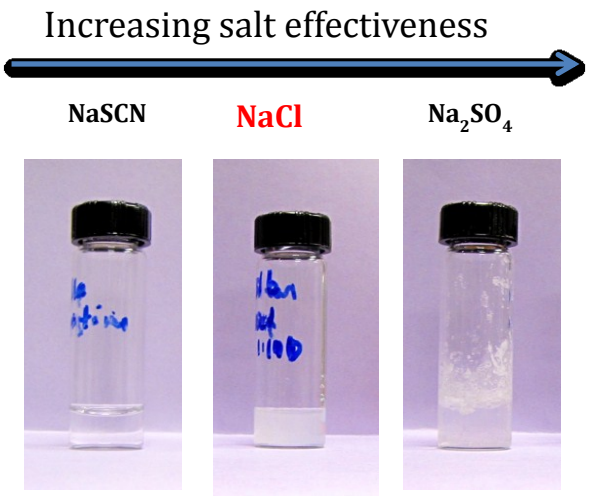

Figure 5. Effect of Salt Type on PVA Aggregation. Na_2SO_4 induces macroscopic aggregates. NaSCN prevents polymer from precipitating. NaCl gives an opaque solution, which indicates the existence of mesoscopic aggregates in the solution.

Turbidity Test

As a further investigation, a turbidity test was performed on the initially transparent PVA (1.1%)-NaCl (2.0 mol/kg)-water sample. The solution becomes cloudier as the temperature is increased from room temperature, as shown in Figure 6. Clarification was observed as the sample was quenched back to room temperature. This reversible phenomenon can be associated with liquid-liquid phase separation (LLPS), also denoted as polymer coacervation. The LLPS temperature was identified by taking the temperature at which the largest turbidity change was observed; i.e. 45 °C.

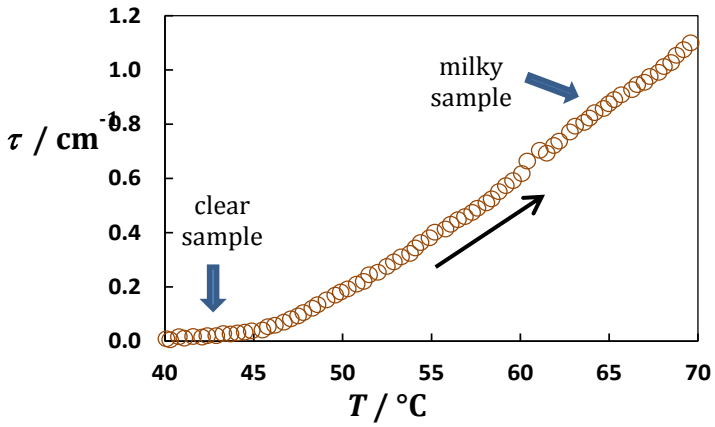

Figure 6. Turbidity Result. The turbidity was plotted as a function of temperature. As temperature increases, the solution becomes cloudier compared to the clear sample observed at room temperature.

Interestingly, after the sample was incubated for five minutes at 95°C and then quenched to 25 °C, the LLPS was no longer observed. We explain this finding by proposing that PVA aqueous solutions already have some polymeric aggregates. It is known that salting-out salts and polymer clustering promote LLPS. However these PVA aggregates can be partially removed by heating samples near the water boiling point. LLPS is no longer observed if the amount of aggregated polymer is reduced. DLS experiments as a function of temperature were used to further examine this phenomenon (see Section 3.5).

Polyvinyl Alcohol (PVA) in Water at 25°C

DLS Representative Distribution of PVA in water (25°C) at a given time is reported in Figure 7. This histogram gives the relative light-scattering contribution of PVA individual chains and PVA aggregates in the solution.

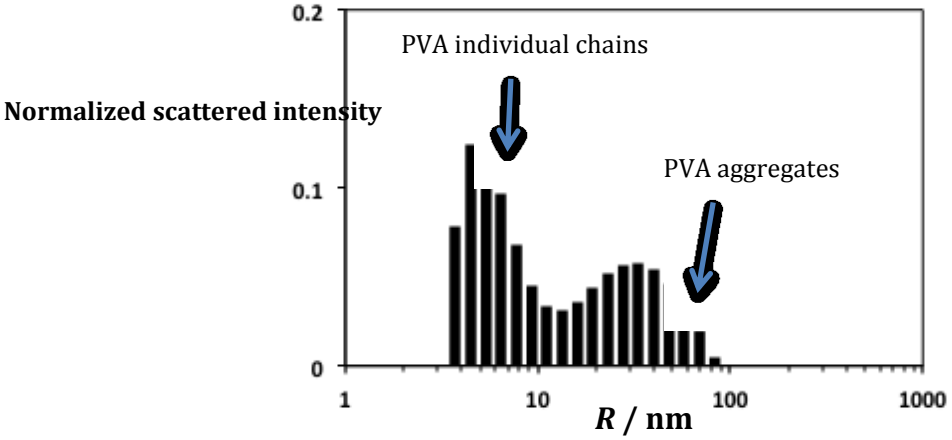

Figure 7. DLS Representative Distribution of PVA in water at 25°C. The y axis gives the normalized scattered-intensity distribution. The x-axis gives R, the radius of particles in nm calculated from diffusion coefficient values. The two peaks of this bimodal distribution represent PVA individual chains and PVA aggregates in the solution.

According to this figure, we can deduce that PVA aggregates are observed in PVA-water solution. The DLS Representative Distributions of PVA in water stay the same throughout time (after one month). Radius of PVA single chains and that of PVA aggregates do not vary with time in PVA water solution either.

Polyvinyl Alcohol (PVA) in NaCl (2M) at 25°C

Figure 8 shows DLS Representative Distributions of PVA in NaCl(2mol/kg) at different representative times and 25°C. Interestingly, the peak of PVA aggregates grows larger and shifts towards higher radii as time increases. In summary, under the effect of NaCl, the amount of aggregated PVA and the aggregate radius are observed to increase.

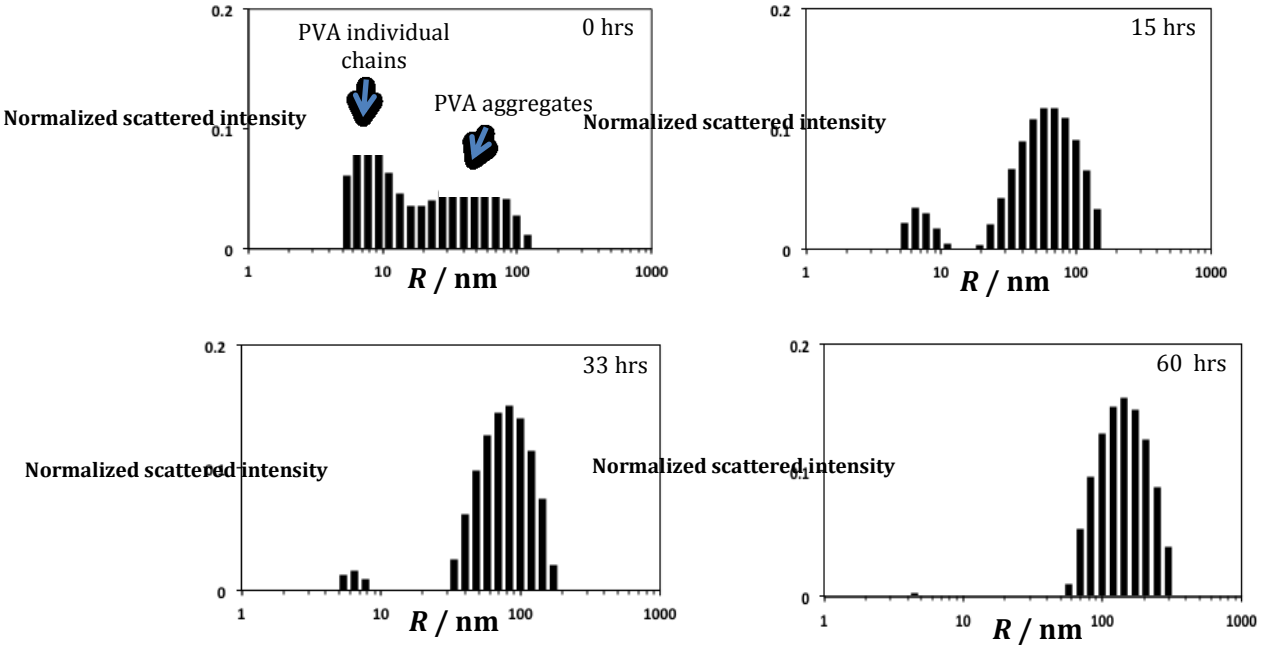

Figure 8. DLS Representative Distributions of PVA(1.1%) in NaCl (2mol/kg) – water at 25°C. Distributions are reported at different representative times: t= 0hrs, 15hrs, 33hrs and 60 hrs. Radius of PVA individual chains is independent of time within the experimental error. On the other hand, radius of PVA aggregate is increasing during the experiment.

From the obtained bimodal distributions, we characterized three independent parameters as a function of time. These are R_{PVA}, R_{agg} and R_{av} where R_{PVA} represents the radius of PVA single chains in the solution; R_{agg} the radius of PVA mesoscopic aggregates, and R_{av} a weighted average between R_{PVA} and R_{agg}. This last quantity gives the relative amount of aggregated PVA in the sample, compared to PVA single chains. Figure 9 shows the values of these three radii throughout time to quantify the kinetic evolution of salt-induced PVA aggregation in PVA (0.5%)-NaCl(2.0 mol/kg)-water solutions at 25°C.

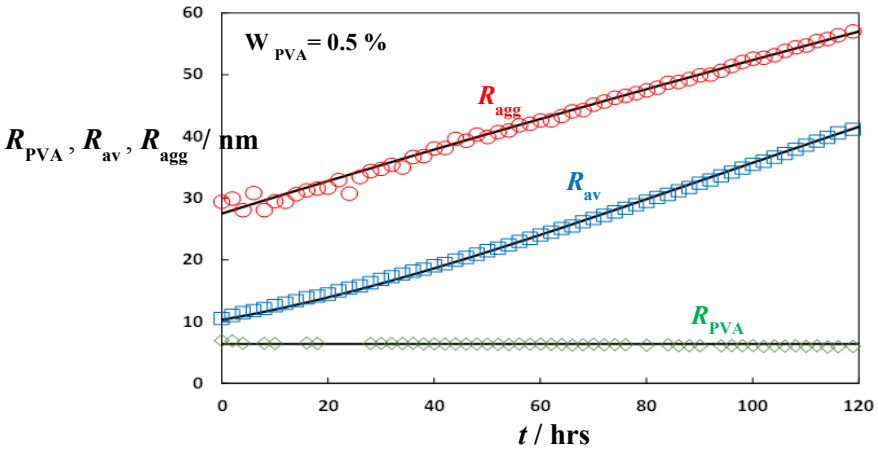

Figure 9. Kinetic Evolution of salt-induced PVA aggregation at 25°C. Radius of aggregates (R_{agg}) and weighted radius (R_{av}) increase with time. On the other hand, radius of PVA single chain (R_{PVA}) stays constant within experimental errors throughout time

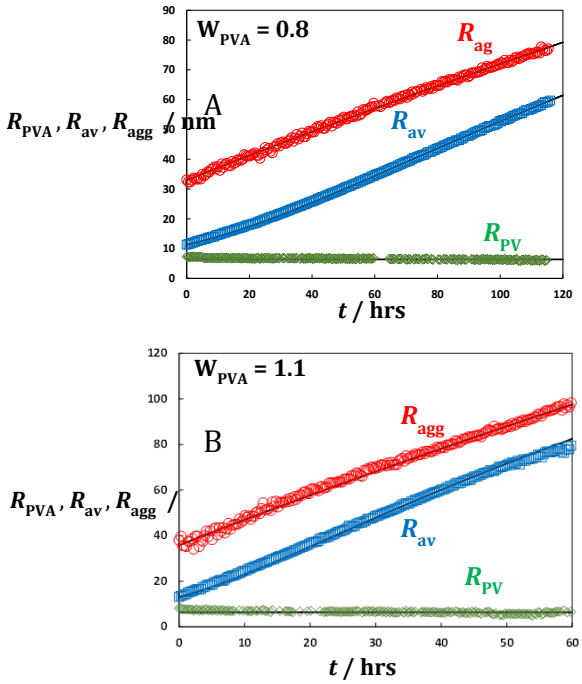

Figure 10. Kinetic results of PVA-NaCl-water solutions with different PVA concentrations (0.8% w/w, A; 1.1% w/w, B).

Radius of PVA single chain is independent of time within the experimental error. On the other hand, R_{agg} is observed to grow with time. R_{av} also increases, indicating that the amount of aggregated PVA increases with time compared to PVA single chains in the solution. The experiment was repeated with two other PVA concentrations 0.8% and 1.1%. Similar patterns were observed; this is shown in Figure 10.

From these experimental observations, we are able to confirm that, without the presence of NaCl, initial aggregates available in the solution will not be able to grow with time. However, aggregates present in PVA-water samples (in the absence of salt) may be critical for observing salt-induced PVA aggregation. Since our turbidity experiment suggests that our PVA aggregates can be reduced by heating, we explore the effects of temperature on PVA aggregation in the following section.

Effect of Temperature on PVA Aggregation

To further evaluate the importance of PVA preexisting aggregates in solution, we conducted two other DLS experiments of PVA-NaCl under different temperature conditions. These experiments give us good insight into the temperature's impact on PVA aggregate formation and growth. Results of these experiments are shown in Figure 11.

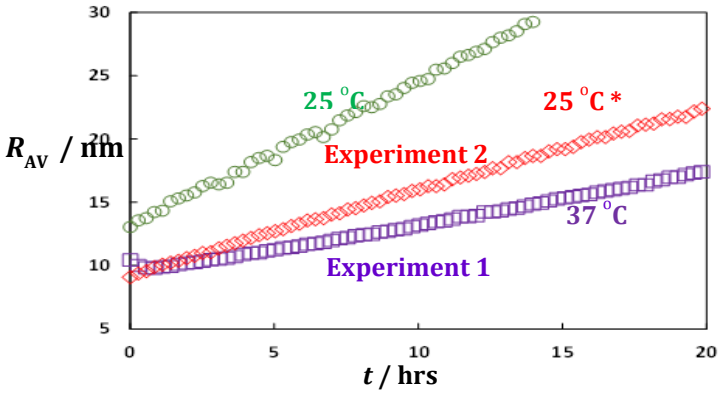

Figure 11. Effect of Temperature on PVA aggregation. Experiment 1 was performed at 37°C. Experiment 2 was performed at 25°C; however the sample was first heated at 95°C for five minutes before running DLS. Compared to the previously-discussed experiments at 25°C, these two experiments show that the initial amount of aggregated PVA is relatively small. The corresponding aggregation rates are also lower.

Experiment 1 was carried out at 37°C. Our results show that the aggregation rate is lower at this temperature compared to 25°C. This is an unusual result since the rate of kinetic processes typically increases with temperature. We explain our findings by observing that the initial amount of aggregated PVA is less at 37°C compared to 25°C. Thus, the amount of preexisting PVA aggregates decrease as temperature increases. To explain the turbidity experiment (see Section 3.2), we performed another DLS experiment in which the sample was first heated at 95°C (for about five minutes) and then quenched to 25°C. DLS experiments on this treated sample were performed at 25°C (Experiment 2). The obtained results were similar to those of experiment 1, thereby confirming that high temperature decreases the amount of initial aggregates available in the solution. Therefore, salt-induced PVA aggregation requires the presence of preexisting PVA aggregates. The effect of NaCl is to trigger their growth.

Light-Microscopy Image of PVA nanoparticles

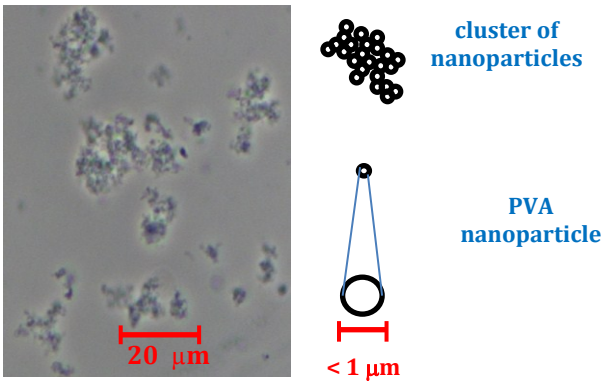

Figure 12. Phase-Contrast Light-Microscopy image of PVA nanoparticles

Phase-contrast Light microscopy was used as an attempt to visualize the PVA aggregates. As shown in Figure 12, clusters of particles with a diameter smaller than 1μm are observed. However, due to the limited resolution of a light

microscope, the morphology of these particles could not be obtained. Nonetheless, this image shows that PVA particles have a diameter falling within the domain of sizes associated with nanoparticles.

In order to characterize the morphology of PVA aggregates, high-resolution electron microscopy should be utilized in future experiments.

DISCUSSION

We will now discuss the kinetic evolution of PVA aggregation by examining our DLS results. Specifically, since DLS measures diffusion coefficients, we consider the mean diffusion coefficient $< D >$ of the bimodal distribution and the mean diffusion coefficients of PVA chains $< D_1 >$ and aggregates $< D_m >$ as a function of time, t. The Stokes-Einstein equation was then used to convert these mean diffusion coefficients into the corresponding equivalent hydrodynamic radii: $< R^{-1} >^{-1}$, $< R_1^{-1} >^{-1}$ and $< R_m^{-1} >^{-1}$, respectively. These parameters were denoted as R_{av}, R_{PVA} and R_{agg} in Section 3 for simplicity.

To quantitatively examine the experimental behaviors, we consider a model for PVA aggregation. This model (shown in Figure 13) is based on the presence of PVA clusters at $t = 0$. Aggregation starts from these clusters and not PVA individual chains. This is consistent with our experimental results, showing the existence of PVA initial aggregates in PVA water solution (Figure 7) and the importance of initial aggregates confirmed in the temperature experiments (Figure 11).

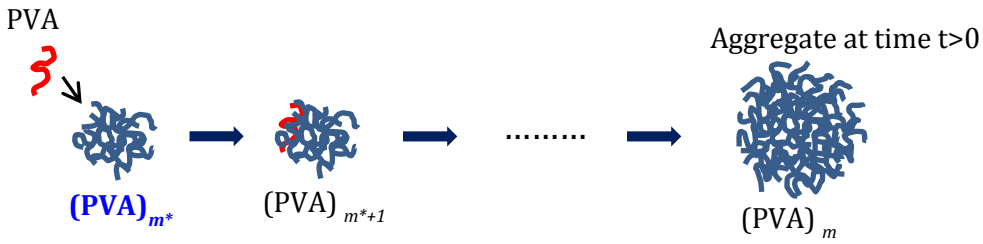

Figure 13. Kinetic mechanism of how PVA aggregates grow. The process starts from initial aggregates $(PVA)_{m^*}$ available in the solution. A PVA chain diffuses towards the initial aggregate creating a bigger aggregate in size $(PVA)_{m^*+1}$. After a definite amount of time, an aggregate $(PVA)_m$ is obtained with a much larger size.

In this model, m^* is the number of PVA chains in the initial aggregate while m is the number of PVA chains in the aggregate at time>0. For simplicity, we will assume these initial clusters to be mono-disperse with aggregation number m^* and molar concentration N_{m^*}. These clusters will irreversibly grow by the stepwise addition of PVA individual chains. We will also assume that PVA individual chains are mono-disperse with a molecular weight of 16 kg/mol**.** The corresponding hydrodynamic radius was set to $< R_1^{-1} >^{-1}$ = 8.4 nm, which was taken as the average of our experimental $< R_1^{-1} >^{-1}$ (values in Table 1).

The irreversible stepwise addition of PVA chains in Figure 13 is described by the following set of reactions:

$$(\mathrm{PVA})_m + \mathrm{PVA} \rightarrow (\mathrm{PVA})_{m+1} \qquad \text{with} \quad m \geq m^*$$

The molar concentration, N_m, of the aggregates with aggregation number m, will evolve according to the second-order kinetic equation:[14]

$$\frac{d N_m}{d t} = C_1 \left(k_{m-1} N_{m-1} - k_m N_m \right) \qquad (2)$$

where $C_1(t)$ is the decreasing molar concentration of free PVA chains and k_m is the second-order kinetic constant describing the formation of $(\mathrm{PVA})_{m+1}$ from $(\mathrm{PVA})_m$. Note that $N_{m^*-1} = 0$ and $k_{m^*-1} = 0$. Concentrations of PVA chains and aggregates are linked by the following mass balance:[14]

$$C_T = C_1(t) + \sum_{m=m^*}^{\infty} m N_m(t) \quad (3)$$

where C_T is the total molar concentration of PVA (see Table 1 for values). Note that $C_T = C_1(0) + m^* N_{m^*}$. The dependence of the kinetic constant, k_m, on m is described by the scaling law: $k_m / k_{m^*} = (m / m^*)^{\beta}$, where β is an exponent to be determined.

In Table 1, we report parameters corresponding to t=0. The values of m* (≈600) were estimated from the corresponding R_{m^*} (≈30 nm) assuming that each aggregate was spherical with a PVA weight fraction corresponding to that of macroscopic hydrogels (14% w/w), and using the specific volume of PVA (0.85 cm^3/g). The values of m^*N_m were then obtained using the following equation valid at t=0:[14]

$$< R^{-1} > = \frac{C_1 R_1^{-1} + m^{*2} N_{m^*} < R_{m^*}^{-1}}{C_1 + m^{*2} + N_{m^*}} \quad (4)$$

Table 1. Experimental Results Obtained from applying Kinetic Model

C_T	$< R^{-1} >^{-1}$	$< R_1^{-1} >^{-1}$	$< R_{m^*}^{-1} >^{-1}$	m^*	C_{PVA}	$m^* N_{m^*}$	$\frac{m^* N_{m^*}}{C}(\%)$	k_{m^*}
mM	nm	nm	nm		mM	μM	%	$\mu M^{-1} hrs^{-1}$
0.353	10.5	8.4	27.5	500	0.352	0.77	0.22	0.032
0.558	11.3	8.4	32.0	690	0.557	1.02	0.18	0.020
0.742	13.2	8.4	35.7	880	0.741	1.49	0.20	0.029

Equation 2 can be solved numerically (using MATLAB) provided that m^*, k_{m^*}, N_{m^*} and β are known. The corresponding $N_m(t)$ solutions can be related to $< R_m^{-1} >^{-1}$, $< R^{-1} >^{-1}$. These can be written as the following weighted averages:[14]

$$< R_m^{-1} >= \frac{\Sigma_{m=m^*}^{\infty} P_m m^2 N_m R_m^{-1}}{\Sigma_{m=m^*}^{\infty} P_m m^2 N_m} \quad (5)$$

$$< R^{-1} >= \frac{C_1 R_1^{-1} + (\Sigma_{m=m^*}^{\infty} P_m m^2 N_m) < R_m^{-1} >}{C_1 + \Sigma_{m=m^*}^{\infty} P_m m^2 N_m} \quad (6)$$

where R_m and P_m are respectively the hydrodynamic radius and the form factor associated with the aggregate $(\mathrm{PVA})_m$. We assume that the aggregate radius follows the following scaling law: $R_m / R_{m^*} = (m / m^*)^{\alpha}$, where α is a radius growth exponent to be determined. Note that α^{-1} represents the fractal dimension of the aggregates. We have already introduced P_m in equation 4 and equation 5, which is the form factor that represents a correction taking into account that the size of the scattering particles (100 nm) cannot be neglected compared to the laser wavelength (633 nm). An expression for the form factor P_m can be obtained by assuming that the

aggregate has spherical symmetry with radius R_m and fractal dimension, α^{-1}. The expression of the form factor is $P_m = [(d / x_m^{1/\alpha}) \int_0^{x_m} x^{(1-3\alpha)/\alpha} \sin x \, dx]^2$, where $x_m \equiv q R_m$ and $q^{-1} = 53.1$ nm, corresponding to the scattering angle of 90°.[14]

The kinetic model based on eq. 2 can be solved numerically provided that m^*, R_{m^*}, k_{m^*}, N_{m^*}, α and β. The values of R_{m^*} and $m^{*\,2} N_{m^*}$ can be directly related to the initial values of $< R^{-1} >^{-1}$ and $< R_m^{-1} >^{-1}$. We can also obtain values of R_{m^*} (=30nm) and $m^{*2} N_{m^*}$ from the calculated values of m^* and N_{m^*} from Table 1.

The value of k_{m^*} / m^* and the exponents α and β can be varied in order to reproduce the experimental shape of $< R^{-1} >^{-1}$, $< R_m^{-1} >^{-1}$. Extracted values of k_{m^*} are reported in Table 1. The value of α that best fits our experimental results at the three PVA concentrations is 0.46. This is higher than a theoretical value of 0.33 corresponding to spherical aggregate with *uniform* structural density. This result implies that PVA aggregates have a relatively low density near their surface compared to their inner core. A picture showing the structure of PVA aggregates is given in Figure 14. The value of *b* that best fits our experimental results at the three PVA concentrations is also 0.46. This is lower than a theoretical value of 0.67 corresponding to spherical aggregate having a density of reactive sites independent of aggregate radius. The obtained value of β implies that density of reactive sites decreases as the aggregate radius increases. Thus the values of α and β are consistent with each other. A picture showing the structure of PVA aggregates is given in Figure 14.

	Radius Growth $R_m = R_{\text{agg},m^*}(m/m^*)^{\alpha}$	Kinetic constant $k_m = k_{m^*}(m/m^*)^{\beta}$
Experimental Value 	0.46 ± 0.03	0.46 ± 0.03
Theoretical value for spherical aggregate with uniform structural density 	0.33	0.67

Figure 14. Extracted Kinetic Parameters. Experimental radius growth exponent α (0.46) is higher than the theoretical value (0.33). And experimental kinetic constant exponent β (0.46) is lower than the theoretical value (0.46). Due to this, we are able to characterize the morphology of our aggregates as less sphere and lower density on the surface to the inner core than the normal aggregates.

The obtained kinetic constants are significantly smaller than those associated with diffusion-limited aggregation. Thus we believe that we have a reaction-limited aggregation. This is shown by the following estimate. We can estimate the diffusion-limited kinetic constant by using:[15]

$$k_{m^*}^{(\mathrm{DLA})} = 4\pi N_A R_{\text{agg},m^*} D_{\mathrm{PVA}} = 2.6 \square 10^7\ \mu\mathrm{M}^{-1}\,\mathrm{hrs}^{-1}$$

This value is several orders of magnitude higher than our k_{m^*} reported in Table 1. The much lower kinetic constant proves that the aggregation process is not limited by the rate of diffusion of PVA chains to the aggregate surface but by PVA incorporation in the aggregate. This process is likely to involve extensive conformational changes of PVA chains upon binding.

CONCLUSION

The Hofmeister series can be used to tune PVA aggregation. While Na_2SO_4 induces macroscopic aggregates, NaSCN inhibits PVA from forming precipitates. PVA mesoscopic aggregates can be observed in aqueous NaCl solution. Initial aggregates (seeds) observed in PVA-water solution are necessary for NaCl induced PVA aggregation. These initial aggregates increase in size in the presence of NaCl. A

kinetic model was used to quantitatively describe our DLS results. Through examination of two extracted kinetic parameters: radius growth exponent α and kinetic constant exponent β, we are able to conclude that our obtained PVA mesoscopic aggregates are not compact and tend to have lower structural density on the surface. Values of kinetic constants are significantly low, for a diffusion-limited aggregation process. This implies that an extensive reorganization of PVA chains and related steric effects play a crucial role in the association process. For future work, higher resolution of electron microscopy is needed to characterize our PVA aggregates. PVA aggregates can be very suitable and can act as a scaffold for other molecules with relevance to drug delivery, as proved by previous works in our lab. Our method to obtain PVA nanoparticles does not involve toxic chemicals and dangerous procedures; indeed it is based on very mild conditions (room temperatures) and utilizes biocompatible chemicals such as PVA and NaCl.

LIST OF REFERENCES

1. M.H. Alves, B.E. Jensen, A.A. Smith, A.N. Zelikin, "Poly(vinyl alcohol) physical hydrogels: new vista on a long serving biomaterial" (**2011**), *Macromol. Biosci. 11*, 1293.
2. B.V. Slaughter, S.S. Khurshid, O.Z. Fisher, A. Khademhosseini, N.A. Peppas, "Hydrogels in regenerative medicine" (**2009**), *Adv. Mater. 21*, 3307.
3. C.M. Hassan, N.A Peppas, "Structure and applications of poly(vinyl alcohol) hydrogels produced by conventional crosslinking or by freezing/thawing methods" (**2000**), *Adv. Polym. Sci. 153*, 37.
4. Y. Zhang; P.S. Cremer, Chemistry of Hofmeister Anions and Osmolytes, *Annu. Rev. Phys. Chem.* **2010**, *61*, 63-83.
5. R. Ricciardi, F. Auriemma, C. Gaillet, C. De Rosa, F. Laupretre, "Investigation of the crystallinity of freeze/thaw poly(vinyl alcohol) hydrogels by different techniques" (**2004**), *Macromolecules 37*, 9510.
6. R. Ricciardi, G. Mangiapia, F. Lo Celso, L. Paduano, R. Triolo, F. Auriemma, C. De Rosa, F. Laupretre, "Structural organization of poly(vinyl alcohol) hydrogels obtained by freezing and thawing techniques: A SANS study" (**2005**), *Chem. Mater. 17*, 1183.
7. H. Noguchi, H. Jyodai, S. Matsuzawa, "Formation of poly(vinyl alcohol) iodine complexes in solution" (**1997**), *J. Pol. Sci., Part B: Polym. Phys. 35*, 1701.
8. M.Z. Liu; R.S. Cheng; C. Wu, R.Y. Qian, "Viscometric investigation of intramolecular hydrogen bonding cohesional entanglement in extremely dilute aqueous solution of poly vinyl alcohol" (**1997**), *J. Pol. Sci., Part B: Polym. Phys. 35*, 2421.
9. Y. Ri-Sheng, Y. Qi-Dong, L. Peng-Ju, Y.F. Xu "Synthesis and pH-induced phase transition behavior of PAA/PVA nanogels in aqueous media" (**2009**), *J. Appl. Polym. Sci. 111*, 358.
10. X. Yang, Y.-Y. Tong, Z.-C. Li, D. Liang, "Aggregation-induced microgelation: a new approach to prepare gels in solution" (**2011**), *Soft Matter 7*, 978.

11. M.A. Gauthier, M.I. Gibson, H.A. Klok, "Synthesis of functional polymers by post-polymerization modification" (**2009**), *Angew. Chem. Int. Ed. Engl. 48*, 48.
12. V.G. Kadajji, V.B. Guru, Water Soluble Polymers for Pharmaceutical Applications, *Polymers* **2011**, *3*, 1972-2009.
13. T. Engel, P. Reid, *Physical Chemistry*, pp.918. [second edition]
14. K.S. Schmitz, *An introduction to Dynamic Light Scattering by Macromolecules* (Academic Press, Boston, 1990)